References

1. Sacconi, S.F. - *The 'Secrets' of Stradivari* (English Edition), Cremona, 1979
2. Möckel, M. - Das Konstructionsgeheimnis der Alten Italienischen Meister, 1925
3. Jolly, V.G. - The Strad, December 1977, pp. 713-719
4. Condax, L.M. - CAS Newsletter #37, May 1982, pp. 31-36
5. White, R. - The Strad, August 1984, pp.258-259; October 1984, pp.437-438
6. Ghisalberti, E.L. - Bee World 60(2), 1979, pp.59-74
7. Fulton, W. - Propolis Violin Varnish, San Diego, California, 1968
8. Knopf, E. & Ogait, A. InstrumBau-Z. 5, 1961, pp.152-160

ON MEASURING WOOD PROPERTIES, PART 2

M. E. McIntyre and J. Woodhouse

Dept. of Applied Mathematics and Theoretical Physics, Silver Street, Cambridge CB3 9EW, U.K.; and
Topexpress Ltd., 13-14 Round Church Street, Cambridge CB5 8AD, U.K.

1: Introduction

In Part 1 of this study [1] we discussed some of the general principles involved in the measurement and interpretation of the elastic and damping constants of wood. It was explained that to characterise a given piece of wood at a given frequency requires measurement of nine elastic constants, each with an associated damping constant, 18 constants in all. For the simplest interesting case, that of a flat, thin, quarter-cut plate, four elastic constants are needed together with four damping constants. We also showed in Part 1 that conventional strip measurements are not able to give all the plate constants, let alone the others, even if strips are cut at angles other than the usual long-grain and cross-grain directions.

Thus the simplest possibility for measuring the 8 constants for a given quarter-cut plate (e.g. the real and imaginary parts of the four complex quantities D_1, D_2, D_3 and D_4 defined in Part 1) would seem to be by interpreting the frequencies and Q-factors of the lower resonant modes of the plate. This is the subject of the present discussion - we describe what can be done with rectangular plates, and illustrate with measurements on two samples. One of these is a specimen of soundboard spruce; the other is a carbon-fibre composite plate somewhat similar to those discussed by Haines et al. [2], and kindly provided by CIBA-GEIGY at Duxford near Cambridge.

Rectangular plates are of interest as a simple case for analysis, but also for a more practical reason. As discussed in Part 1, there is a real need for a systematic programme of measuring material properties on a range of instrument wood. One interesting possibility for such a survey would be to use spruce for guitar fronts, which is usually supplied machine-thicknessed to about 4mm and cut into rectangular plates with an aspect ratio of about 2:1. This offers a ready-made source of specimens to anyone with access to a supplier of materials to guitar-makers, and makes a study of rectangular plates particularly apposite. We shall describe a method by which anyone can get a useful first approximation to seven of the eight constants by simple measurements on the free vibrations of such plates, and also how this method can quite readily be enhanced (for those with access to a computer) to give higher accuracy and to give some estimate of the eighth constant.

2: Measuring the elastic constants

The usual methods of determining elastic moduli include static compression and torsion measurements, ultrasonic wave-speed measurements and strip vibration mode tests. In all of these cases, each individual test yields one elastic modulus by simple substitution into a formula. For the measurements we are about to describe, trying to determine the four elastic constants D_1, D_2, D_3 and D_4 of a flat orthotropic plate (and also the imaginary parts of these four constants), things are unfortunately not so simple. For most of the modes, the frequency is influenced to some degree by all four of the elastic constants. Thus to get the best out of a given set of measurements, we need to solve the full plate-vibration problem. This needs a computer, although not necessarily a very powerful one - in the Appendix we describe a method by which anyone with access to a computer big enough to have a simple scientific subroutine library can very easily write a suitable program.

However, it will turn out that we can get surprisingly far without recourse to a computer. Our method falls into three stages, and computing enters only at stage three. Stages one and two on their own give useful first approximations to the real parts of all four constants, as will be shown in the first half of this section. In section 3 we discuss the parallel problem of using measured Q-factors to determine the imaginary parts of the constants, and in a similar way it will turn out that three of the four can be obtained to a first approximation without the need for computer calculations. The use of a computer can again improve accuracy, and also seems to be necessary in order to gain any useful information on the last of the constants.

The first few vibration modes of an orthotropic rectangular plate with parameters of the right order for soundboard spruce generally look rather like the illustrations in Fig. 1. They are shown here for a square plate, in the

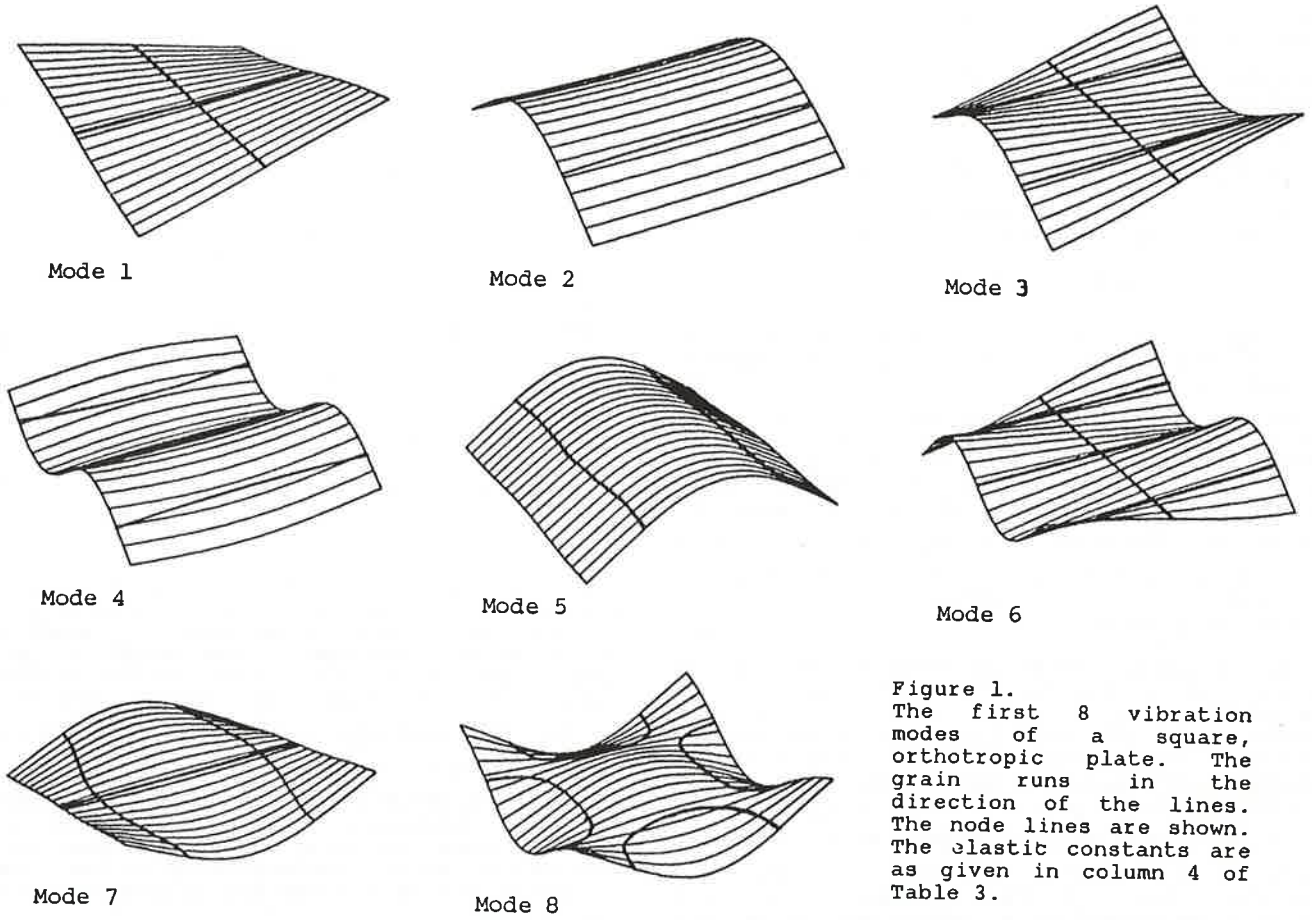

Figure 1.
The first 8 vibration modes of a square, orthotropic plate. The grain runs in the direction of the lines. The node lines are shown. The elastic constants are as given in column 4 of Table 3.

sequence which corresponds to a particular set of values of the elastic constants (in fact those of our carbon-fibre composite plate). With different constants or with a non-square plate the sequence will change, but essentially the same set of modes will still be found. The only significant exception is a well-known one, when the length-to-breadth ratio of the plate is tuned to just the right value (usually about 2:1) so that the two lowest "bar modes" (modes 2 and 5 in Fig. 1) are replaced by a "ring mode" and an "X-mode" [3]. We shall return to this special case shortly.

For stage 1 of the process we pick a plate not tuned to give ring and X modes, and measure the frequencies of the modes corresponding to numbers 1, 2 and 5 in Fig. 1: call these f_1, f_2 and f_5 respectively (all in Hz). Given the mass density ρ of the plate and its dimensions (say a x b, a along the grain and b across, and thickness h), we can now write down formulae which give useful first approximations to the real parts of the constants D_1, D_3 and D_4 (all units are S.I., so that the D's are in Pa i.e. Newtons per square metre):

$$D_1 = 0.0789\ f_5^2\ \rho\ a^4/h^2 \qquad (1)$$

$$D_3 = 0.0789\ f_2^2\ \rho\ b^4/h^2 \qquad (2)$$

$$D_4 = 0.274\ f_1^2\ \rho\ a^2b^2/h^2 \qquad (3)$$

The first two of these are just the familiar formulae used in the strip-testing method [4], but with $12D_1$ and $12D_3$ instead of the long-grain and cross-grain Young's moduli, as explained in §3 of Part 1 [1]. The third formula is the one we calculated in Part 1 as an example of the application of Rayleigh's variational principle, in the discussion following eq. (4). The justification of eqs. (1) and (2) is very similar to that of eq. (3) explained in Part 1: to derive them, one-dimensional gravest bar modes are used as guesses for the plate displacement in Rayleigh's principle. The level of accuracy to be expected from these formulae will emerge later, when we discuss stage 3 and the computer results.

To determine D_2 to a corresponding approximation requires a little more ingenuity. One possibility may occur to readers of Part 1: it was noted there that what one actually measures in the usual long-grain and cross-grain strip tests is not D_1 and D_3, but slightly more complicated combinations of constants involving D_2 as well (see eq. (8) in Part 1). Could we combine strip test results with the estimates of D_1 and D_3 given above to deduce D_2? Unfortunately, this idea does not work. The frequency differences involved, between strip modes and corresponding "bar-like" plate modes, turn out to be extremely small, beyond the scope of accuracy of eqs. (1) and (2) (and incidentally small enough to be hard to measure reliably).

A better method is available, also taking its inspiration from something said in Part 1. We noted there that D_2 has a particularly strong influence on frequencies when the plate is cut so as to have a "ring mode" and an "X-mode". The ring mode invariably has a higher frequency

than the X-mode, and this difference is due almost entirely to the effect of D_2, as was explained below eq. (2) of Part 1. This fact leads to stage 2 of our programme.

By adjusting the aspect ratio of our plate, we can produce these two modes in place of modes like 2 and 5 in Fig. 1. This occurs when the ratio a/b is equal to the fourth root of the ratio of long-grain and cross-grain D's:

$$a/b = (D_1/D_3)^{1/4} \qquad (4)$$

This aspect ratio usually turns out to be about 2:1 for spruce. Of course, this scaling process provides a check on the values of D_1 and D_3 determined in stage 1, by eqs. (1) and (2). Having obtained the ring and X modes, we measure their frequency ratio (and also their Q-values for later reference). From this frequency ratio and the known ratio D_1/D_3 we can then read off the appropriate value of D_2/D_3 from the contour plot given in Fig. 2, which contains all the necessary numerical information for this particular problem.

As a small check at this stage, it is instructive to observe the Chladni patterns of the plate modes. Notice in Fig. 1 that in several cases the node lines are conspicuously curved. This feature, which was readily observable in our plate experiments, is a result of a significantly non-zero value of D_2. Because D_2 is relatively hard to visualise and measure, there is sometimes a tendency to ignore it entirely. Even if the frequencies are not strongly influenced by D_2 (which may or may not be the case in any particular plate), we should not forget that mode shapes matter just as much as frequencies, and these are certainly influenced by D_2.

We have now reached the limit of what can be done without some computer-aided tweaking. This tweaking is stage 3. We first need a program which, given values of D_1, D_2, D_3 and D_4 together with plate dimensions and density, can calculate mode shapes and frequencies. As already mentioned such a program is easily written, and a particularly simple method is described in the Appendix. The first thing to do with such a program is to feed in the values determined in stages 1 and 2, and see how well the frequencies thus predicted agree with those measured on the plate. At this stage, the more frequencies one can measure accurately, the better. Because of the nature of the approximations used in deriving eqs. (1)-(3), the computed frequencies at this stage should slightly overestimate the measured ones. In other words the D's should be underestimated so far. Stage 3 consists of adjusting upwards the estimates of the D's to counteract the slight inaccuracies in eqs. (1)-(3) revealed by running the program. A systematic method of carrying out this adjustment is closely related to the method of deducing damping constants from measured Q-factors, and so it is convenient to defer a detailed explanation until the next section.

In the remainder of this section we look at some results, and see how the method works out in practice. We have used two specimens. One was a plate of Norway spruce, Picea abies, 178mm square, 2.4mm thick and with a density of 415kg/m³. Before being cut down to square, the plate had been adjusted to give the ring and X modes, yielding a frequency ratio 1.19. The

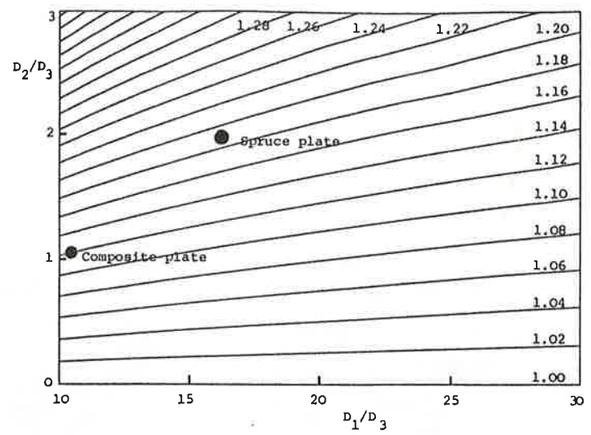

Figure 2. Contour map of the ratio of ring mode frequency to X-mode frequency for a range of the elastic constants of a rectangular, orthotropic plate which encompasses the usual range of properties of spruce. The length-to-breadth ratio of the plate is always scaled to $(D_1/D_3)^{1/4}$. Although it makes little difference to the results, D_4 is always set to $\sqrt{(D_1D_3)}$, to give it a broadly realistic value. The contours of equal frequency ratio are labelled where space permits, and carry on with the same spacing thereafter. Points corresponding to the "simple estimate" values for the two plates tested here are marked.

second specimen used was a plate of composite material, consisting of unidirectional, high-tensile carbon fibres in an epoxy matrix bonded onto each face of a sheet of balsa wood of nominal thickness 1/32". This "sandwich" is somewhat different from that described by Haines et al. [2], who used cardboard as a core material. It should be explained that the properties of this plate did not arise from any systematic attempt to match the properties of any particular wood: rather, they arose simply from the use of standard "pre-preg" carbon fibre tape, and balsa as available from our local model shop. CIBA-GEIGY, who supplied the plate together with some other variations of it, were interested for a time in musical applications of such composites. They arranged to fit a (rather poor) classical guitar with a top made of a material similar to the one tested here, and this is still in our possession. The plate we discuss measured 204mm square and 1.18mm thick, and had an effective volume density of 687kg/m³. When cut down to obtain the ring and X modes, a frequency ratio 1.12 was obtained.

The various frequency data for these two plates are collected up in Table 1. On the left are shown schematic diagrams of the modes measured (but recall from Fig. 1 that the actual node line patterns can differ significantly from such sketches). The first column of numbers shows the measured mode frequencies for both plates. Using eqs. (1)-(3) with the corresponding mode frequencies yields the values of D_1, D_3 and D_4 given in the first and third columns of Table 3, in which all the stages of determining the eight constants for these two plates are summarised. Use of Fig. 2 with these values of D_1/D_3 and the ring-X frequency ratios

Table 1

Mode	Measured frequency	Computed frequency (first estimate)	Computed frequency (final estimate)	Caldersmith
	102	97	102	data
	59	57	59	data
	119	116	119	data
	89	88	89	data
	245	231	241	242
	148	146	150	151
	335	319	328	335
	244	240	244	248
	479	473	479	data
	286	285	286	data
	522	516	525	522
	316	309	312	310
	-	616	633	641
	389	382	388	382

Grain

Frequencies (all in Hz) of the first few modes of the two plates. In each cell, the frequency appropriate to the spruce plate appears above and to the left, and that appropriate to the carbon-fibre composite plate appears below and to the right. The entries marked "data" are the input to Caldersmith's [5] eq. (16).

given above yields the values of D_2 also given in columns 1 and 3 of Table 3. These are our first approximations to the four constants. From these values the computer program gives the frequencies listed in column 2 of Table 1.

It will be seen by comparing columns 1 and 2 of Table 1 that the frequencies are all within striking range of the measurements. The deviations range to just over 5%, suggesting that we have the D's correct to within 10% or so, since frequencies scale with the square root of the D's (eq. (4) of Part 1). This, then, is the level of accuracy we achieve by the simple determination of elastic constants described in stages 1 and 2 above. The result of stage 3 enables us to modify the D's (as will be described in the next section) to produce the values listed in columns 2 and 4 of Table 3. These values, our best-fitted ones, give the frequencies listed in column 3 of Table 1. The match to experiment is now within the limits imposed by experimental techniques and sample inhomogeneity. The carbon-fibre plate, being naturally more uniform than spruce, produces agreement within our frequency-measurement limits. In the spruce plate, agreement is slightly less close, but it was noted during the experiments that this particular spruce plate had significant variations in ring spacing across the plate, leading to very obviously distorted Chladni patterns of some of the modes measured (especially the long-grain bar mode, mode 5 of Fig. 1). Thus some frequency misfit was to be expected.

As an aside on these measurements, in the final column of Table 1 we show frequencies calculated according to the heuristic formula given by Caldersmith [5], his eq. (16). This relates the higher mode frequencies to those of modes 1, 2 and 5 (Fig. 1), and it is interesting to note that this relationship is quite accurate for our plates. Indeed, for our spruce plate it is more accurate than our best-fitted computer predictions! Because the fit is more accurate than the frequency measurements themselves, this last result must be to some extent fortuitous, but the extent of the agreement might bear further investigation.

Table 2

Mode	J_1	J_2	J_3	J_4	Q Measured	Q Initial computed	Q Final computed
	.007	-.001	.043	.951	59	58	60
	.008	.000	.039	.954	68	69	66
	.059	-.121	1.059	.004	40	37	42
	.026	-.052	1.025	.002	96	92	84
	.018	-.016	.284	.714	57	52	55
	.015	-.008	.375	.619	79	77	72
	.065	-.117	1.039	.013	46	38	42
	.054	-.064	1.000	.009	84	93	84
	1.006	-.054	.043	.004	140	123	136
	1.005	-.018	.012	.002	484	449	442
	.833	-.016	.035	.149	117	108	120
	.821	.011	.032	.136	206	248	249
	.309	-.087	.576	.202	-	-	-
	.546	.004	.090	.360	126	136	131
	.628	-.257	.628	.001	51	50	54
	.573	-.147	.573	.001	92	139	118
	.445	.103	.445	.007	81	69	84
	.458	.081	.458	.003	167	173	178

Grain

The most accurate computed J's for the modes of the two plates studied, together with the measured and predicted Q-factors as described in the text. The layout follows Table 1, with the spruce result above the composite plate result in each case.

Table 3

	Spruce: Simple estimates	Spruce: Best estimates	Composite: Simple estimates	Composite: Best estimates
D_1 (MPa)	1300	1340	5500	5570
D_2 "	160	168	560	570
D_3 "	81	85.5	530	543
D_4 "	210	227	820	884
η_1	.0071	.0061	.0021	.00198
η_2	-	-.0045	-	-.0061
η_3	.025	.0216	.011	.0113
η_4	.017	.0164	.015	.0154

The elastic and damping constants for the two plates tested, according to the simple estimation procedures and the computer-aided estimation procedures, as described in the text. In each case the last figure is highly unreliable.

In the same article, Caldersmith also discusses the use of plate modes to deduce elastic constants. His method is superficially similar to our "stage 1", but there is an important difference. Caldersmith assumes that the only relevant constants are the three which appear in the equation of motion of an orthotropic plate. Comparing eq. (A5) of our Part 1 with his eq. (7) and correcting a sign error in the latter, we find the following correspondence between his notation (on the left) and ours (on the right) [6]:

$$D_x = 12D_1 \qquad (5)$$

$$D_y = 12D_3 \qquad (6)$$

$$D_{x,y} = 6(D_2 + D_4) \qquad (7)$$

than the X-mode, and this difference is due almost entirely to the effect of D_2, as was explained below eq. (2) of Part 1. This fact leads to stage 2 of our programme.

By adjusting the aspect ratio of our plate, we can produce these two modes in place of modes like 2 and 5 in Fig. 1. This occurs when the ratio a/b is equal to the fourth root of the ratio of long-grain and cross-grain D's:

$$a/b = (D_1/D_3)^{1/4} \qquad (4)$$

This aspect ratio usually turns out to be about 2:1 for spruce. Of course, this scaling process provides a check on the values of D_1 and D_3 determined in stage 1, by eqs. (1) and (2). Having obtained the ring and X modes, we measure their frequency ratio (and also their Q-values for later reference). From this frequency ratio and the known ratio D_1/D_3 we can then read off the appropriate value of D_2/D_3 from the contour plot given in Fig. 2, which contains all the necessary numerical information for this particular problem.

As a small check at this stage, it is instructive to observe the Chladni patterns of the plate modes. Notice in Fig. 1 that in several cases the node lines are conspicuously curved. This feature, which was readily observable in our plate experiments, is a result of a significantly non-zero value of D_2. Because D_2 is relatively hard to visualise and measure, there is sometimes a tendency to ignore it entirely. Even if the frequencies are not strongly influenced by D_2 (which may or may not be the case in any particular plate), we should not forget that mode shapes matter just as much as frequencies, and these are certainly influenced by D_2.

We have now reached the limit of what can be done without some computer-aided tweaking. This tweaking is stage 3. We first need a program which, given values of D_1, D_2, D_3 and D_4 together with plate dimensions and density, can calculate mode shapes and frequencies. As already mentioned such a program is easily written, and a particularly simple method is described in the Appendix. The first thing to do with such a program is to feed in the values determined in stages 1 and 2, and see how well the frequencies thus predicted agree with those measured on the plate. At this stage, the more frequencies one can measure accurately, the better. Because of the nature of the approximations used in deriving eqs. (1)-(3), the computed frequencies at this stage should slightly overestimate the measured ones. In other words the D's should be underestimated so far. Stage 3 consists of adjusting upwards the estimates of the D's to counteract the slight inaccuracies in eqs. (1)-(3) revealed by running the program. A systematic method of carrying out this adjustment is closely related to the method of deducing damping constants from measured Q-factors, and so it is convenient to defer a detailed explanation until the next section.

In the remainder of this section we look at some results, and see how the method works out in practice. We have used two specimens. One was a plate of Norway spruce, Picea abies, 178mm square, 2.4mm thick and with a density of 415kg/m³. Before being cut down to square, the plate had been adjusted to give the ring and X modes, yielding a frequency ratio 1.19. The

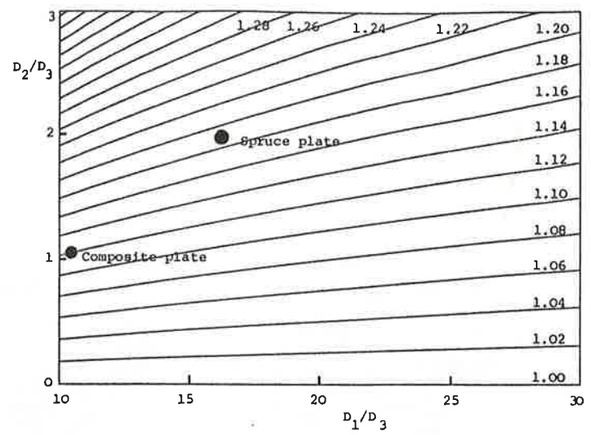

Figure 2. Contour map of the ratio of ring mode frequency to X-mode frequency for a range of the elastic constants of a rectangular, orthotropic plate which encompasses the usual range of properties of spruce. The length-to-breadth ratio of the plate is always scaled to $(D_1/D_3)^{1/4}$. Although it makes little difference to the results, D_4 is always set to $\sqrt{(D_1D_3)}$, to give it a broadly realistic value. The contours of equal frequency ratio are labelled where space permits, and carry on with the same spacing thereafter. Points corresponding to the "simple estimate" values for the two plates tested here are marked.

second specimen used was a plate of composite material, consisting of unidirectional, high-tensile carbon fibres in an epoxy matrix bonded onto each face of a sheet of balsa wood of nominal thickness 1/32". This "sandwich" is somewhat different from that described by Haines et al. [2], who used cardboard as a core material. It should be explained that the properties of this plate did not arise from any systematic attempt to match the properties of any particular wood: rather, they arose simply from the use of standard "pre-preg" carbon fibre tape, and balsa as available from our local model shop. CIBA-GEIGY, who supplied the plate together with some other variations of it, were interested for a time in musical applications of such composites. They arranged to fit a (rather poor) classical guitar with a top made of a material similar to the one tested here, and this is still in our possession. The plate we discuss measured 204mm square and 1.18mm thick, and had an effective volume density of 687kg/m³. When cut down to obtain the ring and X modes, a frequency ratio 1.12 was obtained.

The various frequency data for these two plates are collected up in Table 1. On the left are shown schematic diagrams of the modes measured (but recall from Fig. 1 that the actual node line patterns can differ significantly from such sketches). The first column of numbers shows the measured mode frequencies for both plates. Using eqs. (1)-(3) with the corresponding mode frequencies yields the values of D_1, D_3 and D_4 given in the first and third columns of Table 3, in which all the stages of determining the eight constants for these two plates are summarised. Use of Fig. 2 with these values of D_1/D_3 and the ring-X frequency ratios

Table 1

Mode	Measured frequency	Computed frequency (first estimate)	Computed frequency (final estimate)	Caldersmith
	102	97	102	data
	59	57	59	data
	119	116	119	data
	89	88	89	data
	245	231	241	242
	148	146	150	151
	335	319	328	335
	244	240	244	248
	479	473	479	data
	286	285	286	data
	522	516	525	522
	316	309	312	310
	-	616	633	641
	389	382	388	382

Grain

Frequencies (all in Hz) of the first few modes of the two plates. In each cell, the frequency appropriate to the spruce plate appears above and to the left, and that appropriate to the carbon-fibre composite plate appears below and to the right. The entries marked "data" are the input to Caldersmith's [5] eq. (16).

given above yields the values of D_2 also given in columns 1 and 3 of Table 3. These are our first approximations to the four constants. From these values the computer program gives the frequencies listed in column 2 of Table 1.

It will be seen by comparing columns 1 and 2 of Table 1 that the frequencies are all within striking range of the measurements. The deviations range to just over 5%, suggesting that we have the D's correct to within 10% or so, since frequencies scale with the square root of the D's (eq. (4) of Part 1). This, then, is the level of accuracy we achieve by the simple determination of elastic constants described in stages 1 and 2 above. The result of stage 3 enables us to modify the D's (as will be described in the next section) to produce the values listed in columns 2 and 4 of Table 3. These values, our best-fitted ones, give the frequencies listed in column 3 of Table 1. The match to experiment is now within the limits imposed by experimental techniques and sample inhomogeneity. The carbon-fibre plate, being naturally more uniform than spruce, produces agreement within our frequency-measurement limits. In the spruce plate, agreement is slightly less close, but it was noted during the experiments that this particular spruce plate had significant variations in ring spacing across the plate, leading to very obviously distorted Chladni patterns of some of the modes measured (especially the long-grain bar mode, mode 5 of Fig. 1). Thus some frequency misfit was to be expected.

As an aside on these measurements, in the final column of Table 1 we show frequencies calculated according to the heuristic formula given by Caldersmith [5], his eq. (16). This relates the higher mode frequencies to those of modes 1, 2 and 5 (Fig. 1), and it is interesting to note that this relationship is quite accurate for our plates. Indeed, for our spruce plate it is more accurate than our best-fitted computer predictions! Because the fit is more accurate than the frequency measurements themselves, this last result must be to some extent fortuitous, but the extent of the agreement might bear further investigation.

Table 2

Mode	J_1	J_2	J_3	J_4	Q Measured	Q Initial computed	Q Final computed
	.007	-.001	.043	.951	59	58	60
	.008	.000	.039	.954	68	69	66
	.059	-.121	1.059	.004	40	37	42
	.026	-.052	1.025	.002	96	92	84
	.018	-.016	.284	.714	57	52	55
	.015	-.008	.375	.619	79	77	72
	.065	-.117	1.039	.013	46	38	42
	.054	-.064	1.000	.009	84	93	84
	1.006	-.054	.043	.004	140	123	136
	1.005	-.018	.012	.002	484	449	442
	.833	-.016	.035	.149	117	108	120
	.821	.011	.032	.136	206	248	249
	.309	-.087	.576	.202	-	-	-
	.546	.004	.090	.360	126	136	131
	.628	-.257	.628	.001	51	50	54
	.573	-.147	.573	.001	92	139	118
	.445	.103	.445	.007	81	69	84
	.458	.081	.458	.003	167	173	178

Grain

The most accurate computed J's for the modes of the two plates studied, together with the measured and predicted Q-factors as described in the text. The layout follows Table 1, with the spruce result above the composite plate result in each case.

Table 3

	Spruce: Simple estimates	Spruce: Best estimates	Composite: Simple estimates	Composite: Best estimates
D_1 (MPa)	1300	1340	5500	5570
D_2 "	160	168	560	570
D_3 "	81	85.5	530	543
D_4 "	210	227	820	884
η_1	.0071	.0061	.0021	.00198
η_2	-	-.0045	-	-.0061
η_3	.025	.0216	.011	.0113
η_4	.017	.0164	.015	.0154

The elastic and damping constants for the two plates tested, according to the simple estimation procedures and the computer-aided estimation procedures, as described in the text. In each case the last figure is highly unreliable.

In the same article, Caldersmith also discusses the use of plate modes to deduce elastic constants. His method is superficially similar to our "stage 1", but there is an important difference. Caldersmith assumes that the only relevant constants are the three which appear in the equation of motion of an orthotropic plate. Comparing eq. (A5) of our Part 1 with his eq. (7) and correcting a sign error in the latter, we find the following correspondence between his notation (on the left) and ours (on the right) [6]:

$$D_x = 12D_1 \qquad (5)$$

$$D_y = 12D_3 \qquad (6)$$

$$D_{x,y} = 6(D_2 + D_4) \qquad (7)$$

Caldersmith's formulae for D_x and D_y in terms of the bar modes 2 and 5 in Fig. 1 are the same as our approximate equations (1) and (2). His interpretation of the lowest free-plate mode, however, requires modification. In our notation, his eq. (17) asserts that

$$D_2 + D_4 \approx 0.405\ f_1^2\ \rho a^2 b^2/h^2\ , \qquad (8)$$

which he has argued heuristically on the basis of the high-frequency asymptotic behaviour of the plate equation. By contrast, the computer program confirms what our eq. (3) suggests, that f_1 is determined largely by D_4 alone. It is influenced a little by D_1 and D_3, but hardly at all by variations in D_2 over a large range. By comparing Caldersmith's eq. (17) with our eq. (3), then, we see that the "measurements of $D_{x,y}$" given in his Table II can more accurately be regarded as values, not of $6(D_2 + D_4)$, but of $8.9D_4$ (within the accuracy of our eq. (3)).

3: Measuring the damping constants

We now turn to the use of measured Q-factors to determine the four damping constants, the imaginary parts of the four D's. This is in fact an easier problem theoretically than the determination of the elastic constants from frequencies. The reason is that we can use a small-damping approximation since Q-factors for spruce and related materials are usually large compared with unity. In mathematical language, this makes the problem linear (and computations easier), in contrast to the nonlinear problem relating frequencies to elastic constants.

The result of using the small-damping approximation has already been described in Part 1, and for convenience we reproduce eqs. (5)-(7) from there. The Q-factor of any given vibration mode, with displacement w(x,y) at a point (x,y) on the plate, is given by the relation

$$Q^{-1} = \eta_1 J_1 + \eta_2 J_2 + \eta_3 J_3 + \eta_4 J_4 \qquad (9)$$

where

$$J_1 = \frac{D_1 \iint h^3 w_{xx}^2 dA}{\omega^2 \iint \rho h w^2 dA}, \qquad J_2 = \frac{D_2 \iint h^3 w_{xx} w_{yy} dA}{\omega^2 \iint \rho h w^2 dA},$$

$$J_3 = \frac{D_3 \iint h^3 w_{yy}^2 dA}{\omega^2 \iint \rho h w^2 dA}, \qquad J_4 = \frac{D_4 \iint h^3 w_{xy}^2 dA}{\omega^2 \iint \rho h w^2 dA}\ . \qquad (10)$$

The J's satisfy

$$J_1 + J_2 + J_3 + J_4 = 1\ . \qquad (11)$$

The four dimensionless damping constants η_1, η_2, η_3 and η_4 are simply the ratios of imaginary parts to real parts of D_1, D_2, D_3 and D_4 respectively. The dimensionless numbers J_1, J_2, J_3 and J_4 can be readily computed for each mode.

As before, we can make useful progress by an approximate method which requires no computing. This is best explained by seeing the calculated values of the J's for the modes we have studied. These are shown in Table 2, in a similar format to Table 1 with the values appropriate to the spruce plate and the carbon-fibre plate shown in parallel. The thing we want to note first from this table is that, for both plates, the J's corresponding to our old friends modes 1, 2 and 5 of Fig. 1 have a very simple pattern. Each of these three modes has one of the J's approximately equal to unity, and all the others approximately zero. (This approximation is closely related to that underlying eqs. (1) -(3).) Thus we have an extremely simple way of estimating η_1, η_3 and η_4: they are approximately the reciprocals of the Q-values of modes 5, 2 and 1 (Fig. 1) respectively. There is no mode which comes anywhere near isolating J_2 in a similar way (for reasons made clear in §2 of Part 1). The upshot is that there is no comparably simple way of estimating η_2, even roughly, using these plate modes.

To do better than this, we again resort to the computer. The values given in Table 2 are accurate computations of the J's, using the best estimates of the D's from the previous section. If eq. (9) were exactly satisfied (i.e. our measurements, our computing and the basic theoretical assumptions all precisely right!), we could take any four rows of J and measured Q values from Table 2, and simply solve the four versions of eq. (9) as simultaneous equations to give the four damping constants η_1, η_2, η_3 and η_4. In fact, of course, there will be errors in the measurements if nowhere else. To make best use of all the data we have, we calculate the values of η_1, η_2, η_3 and η_4 which minimise the deviation of all the Q's from the pattern predicted by eq. (9), in a least-squares sense. This leads to a standard "linear regression" problem, which gives us our best estimates of the damping constants.

The results for our two plates are shown in the last three columns of Table 2. These show, first, the measured Q-factors, second, the Q-factors predicted from the simple estimates of η_1, η_3 and η_4 (taking η_2=0) by substituting them into eq. (9) with the accurate J's from Table 2, and, third, the Q-factors given by the linear regression process just mentioned. The values of the η's deduced from these two types of estimate are listed in the lower half of Table 3.

For the spruce plate (upper figures) it will be seen that, as expected, the simple estimate provides a moderately good fit to the data, while the best-fitted values provide a significant improvement. The final values are mostly within experimental tolerances on the Q measurements. (Q's of such light plates require some care to measure, without perturbing the modes significantly or adding extra damping, and it is hard to achieve better than perhaps 5% accuracy.) Even by the linear regression process using data from a number of modes, we do not get very good estimates of η_2. For the spruce plate, the fit to experiment is pretty good if the linear regression is carried out on only three damping constants, setting η_2=0 (results not shown). Putting η_2 in gives a small improvement, particularly to the fit of the ring and X mode Q's, but the value of η_2 thus determined is less certain than those of the other constants. The reason for this difficulty in fixing η_2 is apparent in Table 2, from the smallness of the values of J_2. This may turn out to be a general (and thus useful) fact, that η_2 does not have a significant influence, but our evidence is insufficient to decide the issue. More measurements, and also preferably measurements at higher frequencies, are needed. We shall discuss some of the possibilities (and difficulties) in Part 3.

The measurements on the carbon fibre plate tell a rather different story. For many of the square-plate modes the "best-fitted" η's in fact give a worse fit than the first estimates. What has happened is that the regression process has been heavily influenced by a very poor initial fit to the X-mode, and has reached a compromise which is not a particularly good fit anywhere. If we do not include the ring and X modes in the regression process, a fit to the remaining modes is achieved which is comparable to the agreement shown for the spruce plate. This could mean one of two things. First, there might have been some experimental problem not noticed at the time when the Q measurements on the ring and X modes were made. Second, it is not in any case a priori obvious whether standard plate theory as used here should apply without modification to composite "sandwich" materials like this plate. This is not an issue to pursue here, but merits further investigation. For the moment, we can take the pragmatic view that the frequencies fit the theory very well, while the Q's are rather less convincing (although the general pattern of Q's is well predicted).

Now that we have seen how the J's are used to calculate η's, we can finally explain how stage 3 of the process of fitting elastic constants to frequencies was carried out. The J's are again the key: not only do the J's measure the contribution of each damping constant to the overall modal damping, but they also measure the effect of small changes in the D's on the squared frequency of a given mode. This follows from eq. (4) of Part 1, again using the "insensitivity property" implied by Rayleigh's principle. Thus once we have got a good first approximation to the four D's by stages 1 and 2 described in the previous section, adjusting them to give a more precise fit can be done in a similar way to the simple estimate of η_1, η_3 and η_4 described above: the required ratio of squared frequencies is calculated for the modes 1, 2 and 5 (Fig. 1), and then D_4, D_3 and D_1 respectively are multiplied by those factors. The ratio D_2/D_3 is still fixed by Fig. 2 and the ring-X frequency ratio. If necessary the process can be iterated, recomputing mode frequencies with the new estimates of the elastic constants.

4: Conclusions

We have presented a method for making the best use of the measured frequencies and Q-factors of the low vibration modes of a rectangular orthotropic plate for deducing values of the four elastic constants and four damping constants of the plate. The method has been illustrated by measurements on two materials, a specimen of soundboard spruce and a carbon-fibre composite plate. Agreement between measurements and theory was encouraging, except perhaps for the damping behaviour of the carbon-fibre composite plate, for which there is some question about the applicability of standard plate theory. We have also shown how approximate values of seven of the eight constants may be obtained very easily, without using a computer.

An issue which has been glossed over here is the possible frequency-dependence of the "constants", especially the damping constants. Reasonable agreement with theory has been obtained over the restricted range of frequency used in these measurements (about 100 to 600Hz for the spruce, 60 to 400Hz for the composite plate). For the spruce plate, the main target of the investigation, the agreement is particularly encouraging. It is reasonable to hypothesise that no significant variations with frequency of the properties of the spruce plate have occurred in these ranges. This does not, of course, preclude significant variations at higher frequencies, which are still of interest. Only further measurements at such higher frequencies (presumably by a different approach, a problem we take up in Part 3) will settle the issue.

On the actual measurements made here, we can make a couple of observations. On the spruce, we note that the values of D_1 and D_3 are entirely consistent with the range of values of long-grain and cross-grain Young's modulus reported by Haines for Picea abies [7]. For the carbon-fibre composite plate, at first glance the elastic constants seem to be entirely different from those of spruce. As explained above, no effort was made to match this particular composite to the properties of wood, so this should not necessarily be a surprise. However, we should note that comparing values of D's here is not quite the right thing to be doing. For such a composite "sandwich", taking out the factors of h and h^3 respectively from the kinetic and potential energy expressions (eqs. (2) and (3) of Part 1) is rather artificial. Really, we should compare between the two plates the values of ρh (the area density), which occurs in the kinetic energy, and h^3D_1, h^3D_2, h^3D_3 and h^3D_4, which occur in the potential energy. (These are also more relevant to the coupling to air motion [10].) When the comparison is done on this basis, the composite plate turns out to be far more similar in mechanical properties to the spruce plate.

One final remark to make about the composite plate concerns its Q-factors. It is interesting to note that Haines [2] reported some difficulty in finding a core material giving sufficiently low damping to match spruce. Our plate has gone rather overboard in the opposite direction, with a "long-grain Q" approaching 500! Balsa as a core material may be worth exploring further, since one can always add damping (e.g. by gluing a spruce veneer on top of the composite plate), whereas it is harder to take it away.

Appendix: computing plate modes

When doing the computations for this work, a method of calculating free plate modes was used which is simpler, more reliable and much easier to code than the method described by us previously [8]. It is based on substituting a power series into the Rayleigh quotient, eq. (4) of Part 1, and it takes advantage of the fact that for the particular case of free boundaries, the boundary conditions need not enter the calculations at all. We take as our plate displacement function the expression

$$w(x,y) = \sum_n \sum_m a_{nm} x^n y^m\ , \qquad (A1)$$

and by simple integration, we express the kinetic and potential energy integrals T and V as quadratic forms in the coefficients a_{nm}. One need only use a quarter of the plate, and with the origin at the plate centre the powers in the n and m summations are each taken as either all even or all odd, catering for the four possible cases of symmetry or antisymmetry about the two symmetry axes of the plate. Rayleigh's principle says that V/T is "insensitive to small errors in w", in the sense that it is a stationary function of the quantities a_{nm}. Differentiating V/T with

Caldersmith's formulae for D_x and D_y in terms of the bar modes 2 and 5 in Fig. 1 are the same as our approximate equations (1) and (2). His interpretation of the lowest free-plate mode, however, requires modification. In our notation, his eq. (17) asserts that

$$D_2 + D_4 \approx 0.405\ f_1^2\ \rho a^2 b^2/h^2\ , \qquad (8)$$

which he has argued heuristically on the basis of the high-frequency asymptotic behaviour of the plate equation. By contrast, the computer program confirms what our eq. (3) suggests, that f_1 is determined largely by D_4 alone. It is influenced a little by D_1 and D_3, but hardly at all by variations in D_2 over a large range. By comparing Caldersmith's eq. (17) with our eq. (3), then, we see that the "measurements of $D_{x,y}$" given in his Table II can more accurately be regarded as values, not of $6(D_2 + D_4)$, but of $8.9D_4$ (within the accuracy of our eq. (3)).

3: Measuring the damping constants

We now turn to the use of measured Q-factors to determine the four damping constants, the imaginary parts of the four D's. This is in fact an easier problem theoretically than the determination of the elastic constants from frequencies. The reason is that we can use a small-damping approximation since Q-factors for spruce and related materials are usually large compared with unity. In mathematical language, this makes the problem linear (and computations easier), in contrast to the nonlinear problem relating frequencies to elastic constants.

The result of using the small-damping approximation has already been described in Part 1, and for convenience we reproduce eqs. (5)-(7) from there. The Q-factor of any given vibration mode, with displacement w(x,y) at a point (x,y) on the plate, is given by the relation

$$Q^{-1} = \eta_1 J_1 + \eta_2 J_2 + \eta_3 J_3 + \eta_4 J_4 \qquad (9)$$

where

$$J_1 = \frac{D_1 \iint h^3 w_{xx}^2 dA}{\omega^2 \iint \rho h w^2 dA}, \qquad J_2 = \frac{D_2 \iint h^3 w_{xx} w_{yy} dA}{\omega^2 \iint \rho h w^2 dA},$$

$$J_3 = \frac{D_3 \iint h^3 w_{yy}^2 dA}{\omega^2 \iint \rho h w^2 dA}, \qquad J_4 = \frac{D_4 \iint h^3 w_{xy}^2 dA}{\omega^2 \iint \rho h w^2 dA}\ . \qquad (10)$$

The J's satisfy

$$J_1 + J_2 + J_3 + J_4 = 1\ . \qquad (11)$$

The four dimensionless damping constants η_1, η_2, η_3 and η_4 are simply the ratios of imaginary parts to real parts of D_1, D_2, D_3 and D_4 respectively. The dimensionless numbers J_1, J_2, J_3 and J_4 can be readily computed for each mode.

As before, we can make useful progress by an approximate method which requires no computing. This is best explained by seeing the calculated values of the J's for the modes we have studied. These are shown in Table 2, in a similar format to Table 1 with the values appropriate to the spruce plate and the carbon-fibre plate shown in parallel. The thing we want to note first from this table is that, for both plates, the J's corresponding to our old friends modes 1, 2 and 5 of Fig. 1 have a very simple pattern. Each of these three modes has one of the J's approximately equal to unity, and all the others approximately zero. (This approximation is closely related to that underlying eqs. (1) -(3).) Thus we have an extremely simple way of estimating η_1, η_3 and η_4: they are approximately the reciprocals of the Q-values of modes 5, 2 and 1 (Fig. 1) respectively. There is no mode which comes anywhere near isolating J_2 in a similar way (for reasons made clear in §2 of Part 1). The upshot is that there is no comparably simple way of estimating η_2, even roughly, using these plate modes.

To do better than this, we again resort to the computer. The values given in Table 2 are accurate computations of the J's, using the best estimates of the D's from the previous section. If eq. (9) were exactly satisfied (i.e. our measurements, our computing and the basic theoretical assumptions all precisely right!), we could take any four rows of J and measured Q values from Table 2, and simply solve the four versions of eq. (9) as simultaneous equations to give the four damping constants η_1, η_2, η_3 and η_4. In fact, of course, there will be errors in the measurements if nowhere else. To make best use of all the data we have, we calculate the values of η_1, η_2, η_3 and η_4 which minimise the deviation of all the Q's from the pattern predicted by eq. (9), in a least-squares sense. This leads to a standard "linear regression" problem, which gives us our best estimates of the damping constants.

The results for our two plates are shown in the last three columns of Table 2. These show, first, the measured Q-factors, second, the Q-factors predicted from the simple estimates of η_1, η_3 and η_4 (taking η_2=0) by substituting them into eq. (9) with the accurate J's from Table 2, and, third, the Q-factors given by the linear regression process just mentioned. The values of the η's deduced from these two types of estimate are listed in the lower half of Table 3.

For the spruce plate (upper figures) it will be seen that, as expected, the simple estimate provides a moderately good fit to the data, while the best-fitted values provide a significant improvement. The final values are mostly within experimental tolerances on the Q measurements. (Q's of such light plates require some care to measure, without perturbing the modes significantly or adding extra damping, and it is hard to achieve better than perhaps 5% accuracy.) Even by the linear regression process using data from a number of modes, we do not get very good estimates of η_2. For the spruce plate, the fit to experiment is pretty good if the linear regression is carried out on only three damping constants, setting η_2=0 (results not shown). Putting η_2 in gives a small improvement, particularly to the fit of the ring and X mode Q's, but the value of η_2 thus determined is less certain than those of the other constants. The reason for this difficulty in fixing η_2 is apparent in Table 2, from the smallness of the values of J_2. This may turn out to be a general (and thus useful) fact, that η_2 does not have a significant influence, but our evidence is insufficient to decide the issue. More measurements, and also preferably measurements at higher frequencies, are needed. We shall discuss some of the possibilities (and difficulties) in Part 3.

The measurements on the carbon fibre plate tell a rather different story. For many of the square-plate modes the "best-fitted" η's in fact give a worse fit than the first estimates. What has happened is that the regression process has been heavily influenced by a very poor initial fit to the X-mode, and has reached a compromise which is not a particularly good fit anywhere. If we do not include the ring and X modes in the regression process, a fit to the remaining modes is achieved which is comparable to the agreement shown for the spruce plate. This could mean one of two things. First, there might have been some experimental problem not noticed at the time when the Q measurements on the ring and X modes were made. Second, it is not in any case a priori obvious whether standard plate theory as used here should apply without modification to composite "sandwich" materials like this plate. This is not an issue to pursue here, but merits further investigation. For the moment, we can take the pragmatic view that the frequencies fit the theory very well, while the Q's are rather less convincing (although the general pattern of Q's is well predicted).

Now that we have seen how the J's are used to calculate η's, we can finally explain how stage 3 of the process of fitting elastic constants to frequencies was carried out. The J's are again the key: not only do the J's measure the contribution of each damping constant to the overall modal damping, but they also measure the effect of small changes in the D's on the squared frequency of a given mode. This follows from eq. (4) of Part 1, again using the "insensitivity property" implied by Rayleigh's principle. Thus once we have got a good first approximation to the four D's by stages 1 and 2 described in the previous section, adjusting them to give a more precise fit can be done in a similar way to the simple estimate of η_1, η_3 and η_4 described above: the required ratio of squared frequencies is calculated for the modes 1, 2 and 5 (Fig. 1), and then D_4, D_3 and D_1 respectively are multiplied by those factors. The ratio D_2/D_3 is still fixed by Fig. 2 and the ring-X frequency ratio. If necessary the process can be iterated, recomputing mode frequencies with the new estimates of the elastic constants.

4: Conclusions

We have presented a method for making the best use of the measured frequencies and Q-factors of the low vibration modes of a rectangular orthotropic plate for deducing values of the four elastic constants and four damping constants of the plate. The method has been illustrated by measurements on two materials, a specimen of soundboard spruce and a carbon-fibre composite plate. Agreement between measurements and theory was encouraging, except perhaps for the damping behaviour of the carbon-fibre composite plate, for which there is some question about the applicability of standard plate theory. We have also shown how approximate values of seven of the eight constants may be obtained very easily, without using a computer.

An issue which has been glossed over here is the possible frequency-dependence of the "constants", especially the damping constants. Reasonable agreement with theory has been obtained over the restricted range of frequency used in these measurements (about 100 to 600Hz for the spruce, 60 to 400Hz for the composite plate). For the spruce plate, the main target of the investigation, the agreement is particularly encouraging. It is reasonable to hypothesise that no significant variations with frequency of the properties of the spruce plate have occurred in these ranges. This does not, of course, preclude significant variations at higher frequencies, which are still of interest. Only further measurements at such higher frequencies (presumably by a different approach, a problem we take up in Part 3) will settle the issue.

On the actual measurements made here, we can make a couple of observations. On the spruce, we note that the values of D_1 and D_3 are entirely consistent with the range of values of long-grain and cross-grain Young's modulus reported by Haines for Picea abies [7]. For the carbon-fibre composite plate, at first glance the elastic constants seem to be entirely different from those of spruce. As explained above, no effort was made to match this particular composite to the properties of wood, so this should not necessarily be a surprise. However, we should note that comparing values of D's here is not quite the right thing to be doing. For such a composite "sandwich", taking out the factors of h and h^3 respectively from the kinetic and potential energy expressions (eqs. (2) and (3) of Part 1) is rather artificial. Really, we should compare between the two plates the values of ρh (the area density), which occurs in the kinetic energy, and h^3D_1, h^3D_2, h^3D_3 and h^3D_4, which occur in the potential energy. (These are also more relevant to the coupling to air motion [10].) When the comparison is done on this basis, the composite plate turns out to be far more similar in mechanical properties to the spruce plate.

One final remark to make about the composite plate concerns its Q-factors. It is interesting to note that Haines [2] reported some difficulty in finding a core material giving sufficiently low damping to match spruce. Our plate has gone rather overboard in the opposite direction, with a "long-grain Q" approaching 500! Balsa as a core material may be worth exploring further, since one can always add damping (e.g. by gluing a spruce veneer on top of the composite plate), whereas it is harder to take it away.

Appendix: computing plate modes

When doing the computations for this work, a method of calculating free plate modes was used which is simpler, more reliable and much easier to code than the method described by us previously [8]. It is based on substituting a power series into the Rayleigh quotient, eq. (4) of Part 1, and it takes advantage of the fact that for the particular case of free boundaries, the boundary conditions need not enter the calculations at all. We take as our plate displacement function the expression

$$w(x,y) = \sum_n \sum_m a_{nm} x^n y^m\ , \qquad (A1)$$

and by simple integration, we express the kinetic and potential energy integrals T and V as quadratic forms in the coefficients a_{nm}. One need only use a quarter of the plate, and with the origin at the plate centre the powers in the n and m summations are each taken as either all even or all odd, catering for the four possible cases of symmetry or antisymmetry about the two symmetry axes of the plate. Rayleigh's principle says that V/T is "insensitive to small errors in w", in the sense that it is a stationary function of the quantities a_{nm}. Differentiating V/T with

respect to each non-zero a_{nm} we obtain a set of linear equations which can be solved simply by calling a suitable eigenvalue-eigenvector routine (we used the NAG library routine F02AEF). Free boundary conditions, in all their gory detail (see the Appendix of Part 1), simply "work themselves out" without any effort by the programmer! Mathematically, the reason is that free-boundary modes represent unconstrained stationary points of the Rayleigh quotient. (This is, indeed, the way one works out the form of these boundary conditions [9].)

By varying the order (the number of terms included in the sums over n and m in eq. (A1)), convergence can be tested. For the calculations given here, we used powers up to 11, giving for each symmetry class a 36x36 matrix whose eigenvectors and eigenvalues need to be calculated. At this order, no accuracy problems were encountered using double precision arithmetic. Having thus obtained the modes, it is of course easy to calculate the J's, and these also converged well as the order was increased. The results of this program have been checked against standard textbook results for bars, and against the computations in ref. [8] which were carried out by an entirely different method (finite differences). Anyone interested in a Fortran77 listing for the present method is invited to contact Jim Woodhouse.

References

[1] M. E. McIntyre and J. Woodhouse. On measuring wood properties, Part 1. J. Catgut Acoust Soc. 42 11-15 (1984).

[2] D.W. Haines, C.M. Hutchins, M.A. Hutchins and D.A. Thompson. A violin and a guitar with graphite-epoxy soundboards. Catgut Acoust. Soc. Newsletter 24 25-28 (1975).

[3] The effect will be familiar to readers of this Journal from a number of articles. It is described very clearly for an isotropic plate by Rayleigh (see ref. 9), in art. 226.

[4] J. C. Schelleng. Wood for violins. Catgut Acoust. Soc. Newsletter 37 8-19 (1982).

[5] G. Caldersmith. Vibration theory and wood properties. J. Catgut Acoust. Soc. 42 4-11 (1984).

[6] Caldersmith gives a version of this notation comparison; note that in his version of our eq. (7) he has inadvertantly given a factor 12 instead of 6.

[7] D. W. Haines. On musical instrument wood. Catgut Acoust. Soc. Newsletter 31 23-32 (1979).

[8] M. E. McIntyre and J. Woodhouse. The influence of geometry on linear damping. Acustica 39 209 (1978).

[9] Rayleigh, J.W.S. The theory of sound. Second edition, Macmillan, London (1894) and Dover, New York (1945). See art. 215, below eq. (8).

[10] Schelleng, J. C. The violin as a circuit. J. Acoust. Soc. Am. 35 326-338 (1963) and corrigendum p1291. See section 8.

CORRECTION

An unfortunate omission occurred in the article "A Study of the Effect of String Characteristics on the Performance of the Alto Violin" by Carolyn Wilson Field which appeared in this Journal, No. 42, Nov. 1984.

On page 22 at the bottom of the second column, the last paragraph is herewith reproduced together with the material which should have followed:

> Returning to the balky d'string of the original alto set, the tension it exerted seemed to be undesirably high when compared with its neighboring g and a' strings, as the following table demonstrates.
>
> | Alto Strings Original Set | Designation in Tables I-IV | Tension (lbs) |
> |---|---|---|
> | a' | A-1 | 23 |
> | d' | D-3 | 25 |
> | g | G-1 | 17 |
> | c | C-1 | 17 |
>
> As examples of standard distribution of tensions, new sets of "Dominant" viola and cello strings, tuned to usual pitches, produced the following:
>
> | Viola | Tension (lbs) at 36.5 cm | Cello | Tension (lbs) at 69 cm |
> |---|---|---|---|
> | a' | 17 | a | 29 |
> | d' | 10 | d | 24 |
> | g | 10 | G | 21.5 |
> | c | 9.5 | C | 21.5 |

The text on page 23 follows correctly. Two other corrections should also be noted.

--Page 22, top of second column, the first word should be: Frequency

--Table II, D-9, should be: treble viol

MAKING A SANDING WHEEL

Louis R. Supek
2809 Alda Parkway
Brunswick, Ohio 44212

Planing and scraping a finely framed rib almost to completion and then having it break leads to exasperation. This type of frustration can be alleviated by the use of a sanding wheel.

Items required are:

1. Electric Motor
2. Baseboard
3. Arbor-
4. Sanding Wheel
5. Work Block
6. Hinge, Wood Screws, Carriage Bolt, Compression Spring, Wing Nut and Washer.

1. Electric Motor - Motors are available from discarded washing machines, clothes dryers, furnace blowers and appliance repair shops. Most motors have mounting plates. Furnace blowers have an adjusting bolt and nut to take up slack in a slipping belt. Some motors have provisions for changing shaft rotation by transposing the electrical connections located under the cover plate.

2. Baseboard - A plank about 1 to 1-1/2 inch thick, its length and width to suit the size of the motor mounting plate.

3. Arbor - For mounting the sanding wheel to the motor shaft. They are 1/2 or 5/8 inch in diameter and have right or left handed threads with long or short arbor shafts. Set screws are used to secure the arbor to the motor shaft.

4. Sanding Wheel - A wheel diameter of 4 to 5 inches is sufficient. Made from two pieces of 3/4 inch thick wood and glued together with the grain running at right angles to each other.

5. Work Block - A piece of hardwood a little wider than the width of the sanding wheel. Its length with the hinge flush mounted is equal to the width of the baseboard. The block height clears the bottom of the sanding wheel about 1/16 inch after the wheel has been sanded smooth.

Prepare the work block by removing a square section from the top end of the block about one-half of its thickness. At the bottom end, cut out a section for flush mounting the hinge. Lengthwise, near one edge of the top, cut a slot with a table saw. The groove is used in sanding the lining strip edges. The depth is such that the strip edge just touches the bottom of the sanding wheel, when the spring is compressed.

With the rough cut sanding wheel and arbor attached to the motor shaft, mount the motor to the baseboard. Secure the hinge to the baseboard with short, flat-head wood screws.

At the center of the square section of the block, drill a hole to clear a 1/4-20 carriage bolt. At the bottom of the baseboard drill a shallow recess hole for the head of the bolt. Press the bolt into the wood. The length of the bolt with wing nut and washer should not extend above the level surface of the work block.

Remove the sanding wheel and arbor from the motor shaft. Drill a small pilot hole through the block and baseboard directly under the centerline of the motor shaft. Remove the block from the baseboard and drill a hole slightly larger in diameter than the diameter of the spring and make a shallow recess hole into the top of the baseboard using the pilot hole as a guide. Make the same size hole into the bottom of the work block, its depth to match the length of the spring when compressed.

Insert the spring into the recessed holes and secure the work block to the baseboard. Install the washer and wing nut to the top of the carriage bolt. Turn down the wing nut to compress the spring. No gap should show between the work block and the baseboard.

Insert a piece of sandpaper or emery cloth under the wheel, grit side up, turn on the motor and pull the sandpaper or cloth smoothly and evenly under the wheel to remove any irregularities. Use a vacuum cleaner with hose attached near the wheel to collect the dust particles. Do not breathe into the lungs.

When the wheel is smooth and true, remove the dust particles from the wheel with a cloth and apply the adhesive paper to the wheel. Make the ends into a butt joint. If emery cloth is used, a slot is cut across the wheel surface and the ends of the cloth inserted into the slot and held by a small wedge tapped below the surface of the wheel.

Sand all the ribs on both sides with one setting of the sanding wheel. Make as many passes as necessary to meet the final thickness. Use a micrometer to monitor the thickness at all times. Lining strips are sanded in the same manner.

Other wheel diameters can be made to sand bassbars, neck blocks, etc. Use the wheel for hollow grinding plane blades, knives, chisels and making shims. A grit wheel can be substituted for more drastic grinding of metal strips.

SANDING WHEEL

1. Electric Motor
2. Baseboard
3. Arbor
4. Sanding Wheel
5. Work Block

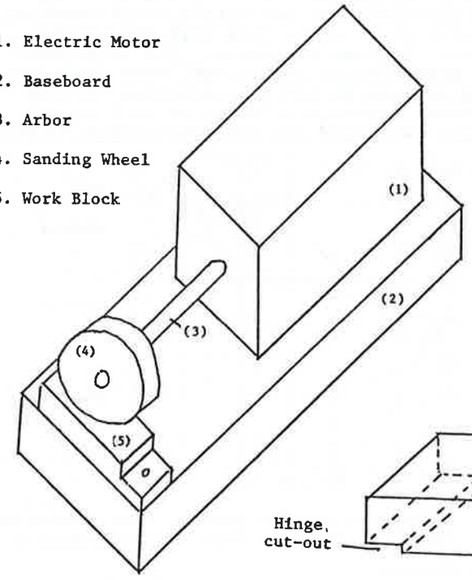

Block Diagram
(not to scale)

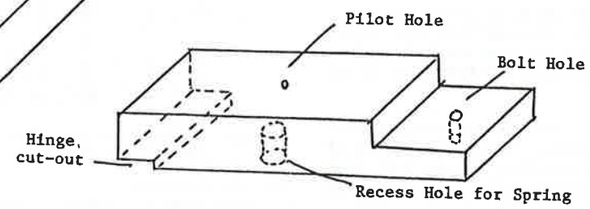

Work Block Detail
Lining Groove not shown

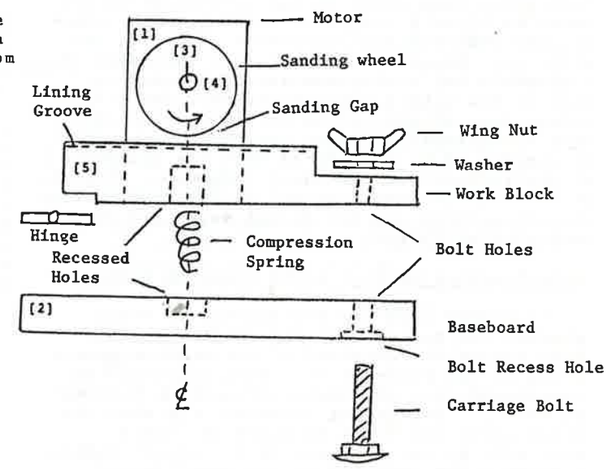

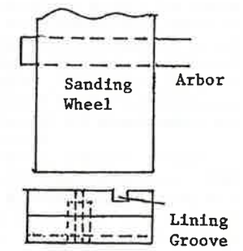

End view
of Block